The Institute of Astronomy & Geophysics
of Mongolian Academy of Sciences

# Book of Extended Abstracts

## The International Conference on Astronomy and Geophysics in Mongolia, 2017

Ulaanbaatar, Mongolia
20-22 July, 2017

1957-2017
60 YEARS

# PROCEEDINGS OF THE INTERNATIONAL CONFERENCE ON ASTRONOMY & GEOPHYSICS IN MONGOLIA, 2017

20-22 JULY, 2017, ULAANBAATAR, MONGOLIA

**Extended Abstract Volume**


Editors in chief

*(Institute of Astronomy and Geophysics, Ulaanbaatar, Mongolia)*

**Prof. Demberel Sodnomsambuu**

**Dr. Odonbaatar Chimed**

**Dr. Ulziibat Munkhuu**



Ulaanbaatar
2017

DDC
551.22
P-23

**INSTITUTE OF ASTRONOMY AND GEOPHYSICS OF MONGOLIAN ACADEMY OF SCIENCES (IAG, MAS)**

Editors: Dr Odonbaatar Chimed
Dr Munkhsaikhan Adiya
Mrs Ankhtsetseg Dorjsuren

Print design: Mungunshagai Mendbayar

**ISBN 978-99978-1-236-0**

Published by Mongol Altay printing Co.ltd

# DEEP STRUCTURE OF THE BAIKAL RIFT SYSTEM BASED ON THE SEISMIC WAVE ATTENUATION

**Anna A. Dobrynina[1,2], Vladimir A. Sankov[1] and Vladimir Chechelnitsky[3]**

[1] *Institute of the Earth's crust of the Siberian branch of the Russian academy of sciences, Irkutsk, Russia*
[2] *Geological institute of the Siberian branch of the Russian academy of sciences, Ulan-Ude, Russia*
[3] *Baikal regional seismological center of Geophysical survey of the Russian academy of sciences, Irkutsk, Russia*

***Contact:*** *dobrynina@crust.irk.ru*

**Abstract**

The investigation data on seismic wave attenuation in the lithosphere and upper mantle of the northeastern flank of the Baikal rift system obtained with a seismic coda envelope and sliding window are considered. Eleven local districts were described by one-dimensional attenuation models characterized by alternation of high and low attenuation layers, which are consistent with the results obtained previously by Yu.F. Kopnichev for the southwestern flank of the Baikal rift system. The subcrust of the lithosphere contains a thin layer with high attenuation of seismic waves likely related to higher heterogeneity (fragmentation) and occurrence of fluids. The lithosphere basement depth varies from 100–120$km$ in the west within the Baikal folded area to 120–140$km$ in the east within the Siberian Platform. It is concluded that there are two asthenosphere layers. Based on specific features of the lithosphere and upper mantle structure, it can be assumed that they were subject to gradual modification involving fluidization processes and partial melting in the Late Cenozoic extension under the influence of distant tectogenesis sources.

## Introduction

To date, it has been proved by a sufficient amount of data that there is no single large mantle anomaly under the Baikal rift system ($BRS$). Thus, the active rifting hypothesis [1] fails to explain fully the forma tion of rift structures. In this connection, it can be sug gested that the extension caused by nonlocal distant sources of tectonic forces [2, 3] initiates gradual changes in the lithosphere properties throughout the section. They are observed as local anomalies expressed, in particular, as deep variations in seismic wave attenuation and velocities.

This paper considers the results of our investigation of deep variations in seismic coda wave attenuation in the lithosphere and upper mantle of the $BRS$ north eastern flank. Previously, based on coda waves of regional earthquakes, we calculated a seismic quality factor of the lithosphere throughout the $BRS$ north eastern flank and compared the results obtained with the crust consolidation age, degree of seismic activity, and faulting [4, 5]. The few works of predecessors investigating the quality factor ($Q$) of the $BRS$ crust and upper mantle, in particular, the northeastern flank, were mostly local in nature. A few publications on this subject can be mentioned [6–8]. Yu.F. Kopnichev [9] studied attenuation regularities in the lithosphere of the $BRS$ southwestern flank and estimated the degree of absorption based on the data of distant stations over the whole region. In general, the regularities of deep variations in the seismic quality factor for the major part of the region are still poorly investigated.

## Method and data

Depth sections with a seismic quality factor $Qc$ were obtained by using coda waves of moderate and strong local earthquakes (twenty events with a magnitude of $M \geq 4$ recorded at an epicentral distance of up to 200$km$, Fig. 1). The data were processed by two methods, such as the seismic coda envelope [6, 9] and the sliding window (the window length was chosen to be 10–15$s$ with a step –5$s$). The coda wave penetration depth was calculated by the standard approach based on simple geometric considerations [10]. The $Q$-value at a frequency of 1$Hz$ was used to analyze deep

variations in attenuation, because the attenuation field heterogeneity is best defined at this very frequency [9].

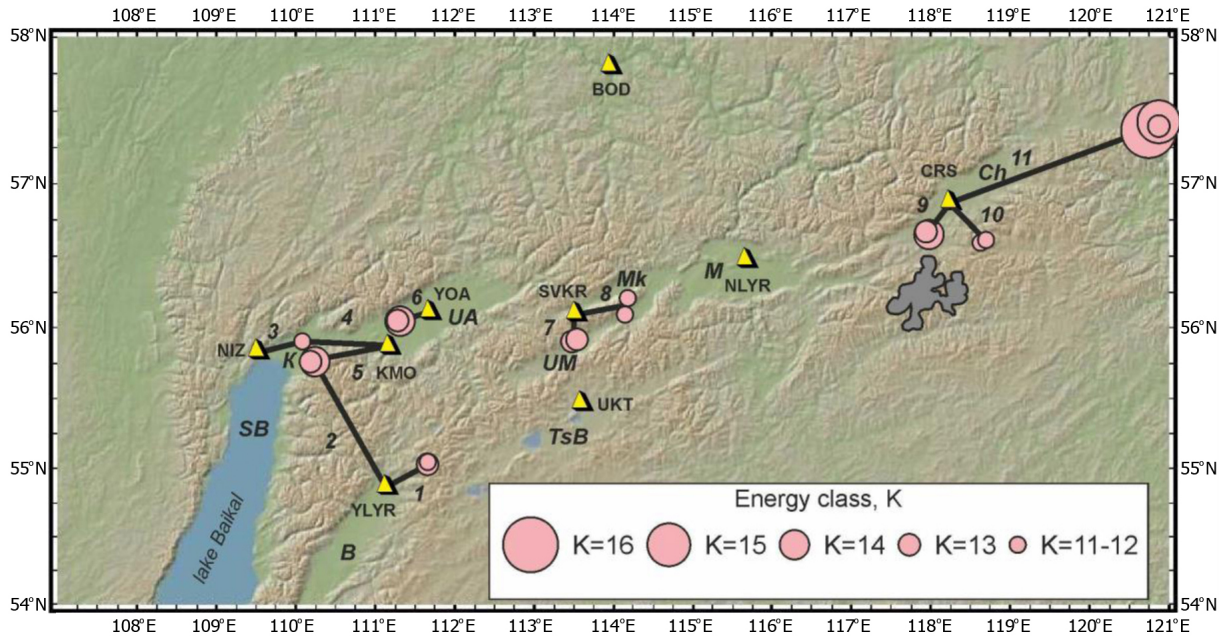


*Figure 1: The position of seismic profiles in the studied region. Seismic stations are indicated with triangles, the position of sections is shown with black lines, the number of sections is indicated with figures, and Cenozoic rift depressions are shown with letters: (K) Kichera, (UA) Verkhneangarsk, (NB) North Baikal, (B) Barguzin, (TsB) Tsipa-Baunt, (UM) Upper Muya, (Mk) Muyakan, (M) Muya, (Ch) Chara. The Udokan basalt field is shown in dark gray.*

## Results

As a result, we obtained one-dimensional depth sections of a seismic quality factor $Qc$ for eleven local areas in the region considered (Fig.2). The depth range was about $260km$ (from 44 to $306km$) and included the lithospheric mantle and asthenosphere (Figs.2). $Qc$ depth sections are indicative of relatively high variations in the quality factor (from 50 to 170) at an irregular change in the $Qc$ value with depth due to alternation of layers with a higher and lower attenuation (Fig.2). Previously, we noted the confinement of changes in attenuation characteristics to velocity boundaries in the lithosphere [4, 5]. At a depth of about $100km$, almost all profiles are characterized by the occurrence of a thin layer (depth of more than $20km$) with a higher attenuation (Fig.2); the layer location depth and thickness are somewhat different at different stations. For instance, at the Ulyunkhan station (YLYR, profiles 1, 2) located on the northern closure of the Barguzin depression, this layer is located at a depth from 70 to $90km$ (profile 1) and from 90 to $100km$ (profile 2). Under the Kichera depression (Nizhneangarsk station, $NIZ$, profile 3), the layer lies at a depth of 110–$140km$; under the Kichera–Verkhneangarsk interdepression spure (Kumora station, $KMO$, profile 5), it gets somewhat thinner and is noted at a depth of 100–$120km$. The higher attenuation layer begins at a depth of $115km$ under the Verkhnengarsk depression (Yoyan station, $YOA$, profile 6), and it rises to a depth of100–$110km$ under the Verkhneangarsk–Muya spur (Severomuisk station, $SVKR$, profiles 7, 8). The Chara depression and its mountain framing (Chara station, $CRS$, profiles 9, 10, 11) are characterized by the deepest position of the roof of the higher attenuation layer such as 120–$140km$. A fairly thick layer of higher attenuation of seismic waves is also located in the section bottom under a few stations. It lies at a depth of 160–$200km$ in the western part of the considered area and at a depth of 180–$240km$ in the east. It should be noted that the higher attenuation of seismic waves is typical of the section top (depth of less than $100km$). According to the measurement data, the lithosphere of the Verkhneangarsk–Muya spur (Severomuisk station, $SVKR$, profiles 7, 8) is characterized by a

layer with the lowest seismic quality coefficient ($Qc(profile7) = 56$, $Qc(profile8) = 68$), right under the crust, at a depth of less than $75km$. Previously, the high attenuation of seismic waves in this area was noted by estimation of the effective quality factor of the lithosphere [4] and was related to the high degree of medium heterogeneity. Profiles 9 and 10 (Chara station, $CRS$) characterizing the lithosphere in the southern part of the Chara depression and north of the Udokan uplift are also indicative of layers with a higher attenuation within the depths of 60–$100km$.

## Discussion

The deep structure of the lithosphere and upper mantle in the studied region was considered in [11–14]. As follows from the analysis data on velocity anomalies of P-waves obtained by 2D teleseismic tomography along the strike of $BRS$ [13], the boundary between negative and positive anomalies of seismic wave velocities is traced under many structures of the rift system at depths of 90–$110km$. This information is in compliance with our data on the location depth of the higher attenuation layer. Alongside with that, it should be noted that under the Chara depression and its mountain framing, the roof of this layer is immersed to a depth of 120–$140km$ in consistency with the higher thickness of the lithosphere in the transition from the folded area to the Siberian Platform. According to the deep seismic sounding data, the low-velocity mantle area is characterized by a two-layered structure [11]. An abnormal subcrustal layer of 20–$50km$ in thickness is separated from deeper levels of the upper mantle with similar velocity characteristics (7.6–$7.8km/s$) by a layer with normal wave velocities typical of this depth (8.0–$8.1km/s$). The difference in a quality factor $Qc$ between these layers ranges from 15–20 to 30–50. According to the magnetotelluric sounding data [12], the studied region hosts a conducting asthenosphere layer at a depth of 80–$120km$ corresponding to a layer with a lower velocity of seismic waves. According to [12], it was formed due to partial melting of mantle rocks. The data given in [15] are in good compliance with our information on the lithosphere foot depth obtained by seismic tomography.

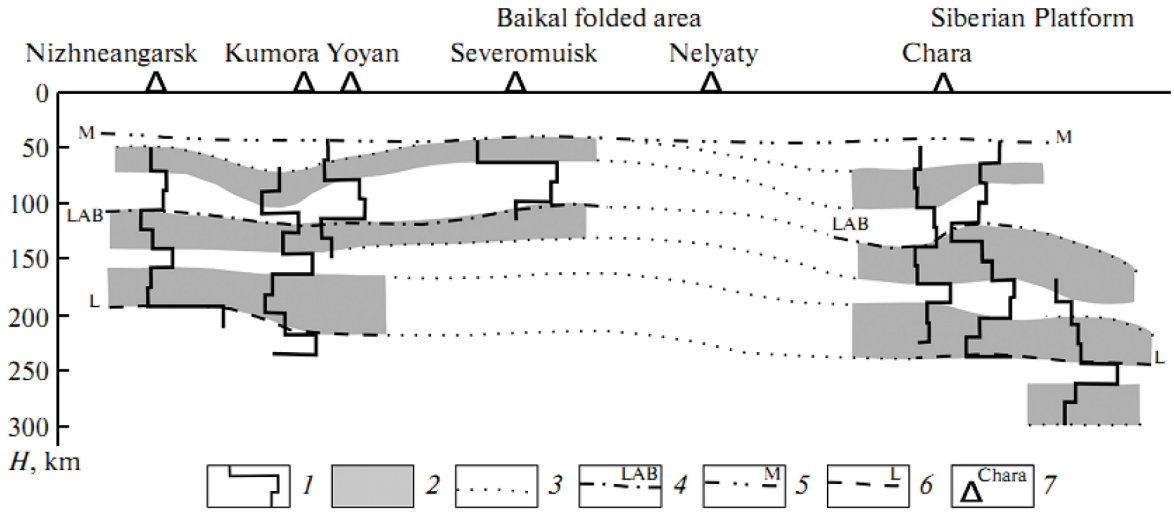


*Figure 2: Schematic section of the lithosphere and upper mantle of the BRS northeastern flank based on the interpolation of data on the absorption of seismic coda waves. (1) seismic quality factor curves; (2) areas with a higher attenuation of seismic waves; (3) assumed boundaries of higher attenuation area; (4) boundary between lithosphere and asthenosphere (LAB); (5) Moho boundary (M) [11]; (6) Lehmann boundary (L); (7) seismic stations and their names.*

As is seen when comparing the obtained $Qc$ sections with one-dimensional profiles of $S$-wave velocities [14], variations in the quality factor values are confined to the velocity boundaries of the medium and areas with higher seismic wave velocities are also characterized by higher $Qc$ values and vice versa (Fig.2). Both methods indicate a three-layer structure of the asthenosphere in the region. The lower boundary of the area with a lower velocity and higher attenuation of seismic

waves in the mantle (Lehmann border) is located at a depth of 190–240$km$. Layers with a higher attenuation of seismic coda waves in the lithosphere (depth of less than 100$km$) recorded within the Verkhneangarsk–Muya spur and in the Chara depression likely have a different origin. In the first case, their formation can be related to higher seismic activity, fragmentation, and, consequently, elevated fluid saturation of the lithosphere. In the second case, we should not rule out the occurrence of intermediate magma chambers—sources of Late Cenozoic basalts at the Udokan volcanic field—at the depth of 70–90$km$ and confinement of higher seismic wave attenuation areas to them. In addition, lithosphere thinning observed under the Udokan field may also be indicative of a melting area in the upper mantle.

Hence, we obtained a multilayered model of the seismic quality factor of the lithosphere and upper mantle in the $BRS$ northeastern flank with alternating layers with a higher and lower seismic wave attenuation (Fig.2). The asthenosphere located at a depth of 90–150$km$ in the region corresponds to layers with a higher attenuation in the section bottom. In addition, one more layer with a higher attenuation identified at a depth of 180–240$km$ can also be interpreted as a part of the asthenosphere. The higher wave attenuation in these layers is most likely related to heterogeneities as horizontal boundaries and to partial melting of the mantle material. The occurrence of layers with a higher attenuation in the section top may be due to high seismic activity, tectonic fragmentation, and fluid saturation of the lithosphere, and also due to the occurrence of magmatic chambers in the lithosphere within the Udokan volcanic field.

## Conclusion

The model of formation of the Baikal rift due to uplifting of a consolidated anomalous mantle body to the lithosphere foot and spreading around proposed previously in [1] assumes the occurrence of a thick layer in all sections, which is characterized by a higher attenuation under the basement of the lithosphere getting thinner. According to our data and [13, 14], there is no consolidated body under the lithosphere of the BRS northeastern flank. The lithospheric and asthenospheric mantle is characterized by a layered structure preventing the convection. The resulting multilayered model of the seismic quality factor of the lithosphere and upper mantle of the BRS northeastern flank together with analogous results for the southwestern flank [9] may be indicative of passive formation of the rift system.

This work was supported by the Russian Foundation for Basic Research (project no. 17-05-00826).

## References

[1] N. A. Logatchev and Yu. A. Zorin, Tectonophysics 143(2), 225–234 (1987).

[2] P. Molnar and P. Tapponier, Science 189, 1959–1982 (1975).

[3] V. A. Sankov, A. V. Parfeevets, A. V. Lukhnev, A. I.Miroshnichenko, and S. V. Ashurkov, Geotectonics 45 (5), 378–393 (2011).

[4] A. A. Dobrynina, V. V. Chechelnitsky, and V. A. Sankov, Lithosphere Quality Factor and Focal Parameters of Earthquakes in the Baikal Region (LAP LAMBERT Acad. Publ., Saarbrücken, 2014).

[5] A. A. Dobrynina, Phys. Earth Planet. Inter. 188, 121–126 (2011). doi:10.1016/j.pepi.2011.05.008

[6] T. G. Rautian, V. I. Khalturin, and M. S. Zakirov, Experimental Investigations of Seismic Code (Nauka, Moscow, 1981) [in Russian].

[7] A. A. Dergachev, Geol. Geofiz., No. 6, 94–101 (1982).

[8] V. M. Kochetkov, N. S. Borovik, A. V. Solonenko, et al., "Detailed seismological studies in North-Muiskii region," in Geology and Seismic Intensity in Baikal-Amur Mainline Region. Seismicity, Ed. by S. L. Solov'ev (Nauka, Novosibirsk, 1985), pp. 123–178 [in Russian].

[9] Yu. F. Kopnichev, Dokl. Akad. Nauk 325 (5), 944–948 (1992).

[10] J. Pulli, Bull. Seismol. Soc. Am. 74, 1149–1166 (1984).

[11] S. V. Krylov, B. P. Mishen'kin, Z. R. Mishen'kina, et al., Lithosphere Detailed Seismological Studies at P- and S-Wavelengths (Nauka, Novosibirsk, 1993) [in Russian].

[12] A. V. Pospeev, "Electrical conductivity of the Earth crust and mantle in the western part of Baikal-Amur region," in Asthenosphere according to Geophysical Methods (Naukova Dumka, Kiev, 1988), pp. 34–44 [in Russian].

[13] V. V. Mordvinova, Extended Abstract of Doctoral Dissertation in Geology and Mineralogy (Institute of the Earth's Crust Siberian Branch Russ. Acad. Sci., Irkutsk, 2009).

[14] L. V. Anan'in, V. V. Mordvinova, M. F. Gots', M. Kanao, V. D. Suvorov, G. I. Tat'kov, and Ts. A. Tubanov, Dokl. Earth Sci. 428 (7), 1067–1070 (2009).

[15] K. Priestley, E. Debayle, D. McKenzie, et al., J. Geophys. Res. 3, B10304 (2006). doi:10.1029/2005JB004082

# CONTENTS


***Astronomy, astrophysics and space science . . . . . 09***

*Owl telescope in Mongolia . . . . . 11*

*Observation of the coronal green line at a wavelength of 5303Å . . . . . 12*

*The results of wavelet analysis application to variations of the Earth rotation parameters . . . . . 13*

*Observation of solar radio bursts . . . . . 14*

*The minor planets in the solar system . . . . . 15*

*Intensity of solar ultraviolet radiation in Ulaanbaatar regions and comparative analysis of some characteristics of climatic conditions in the places of Khurel-Togoot and Tavan tolgoi . . . . . 16*

*A fuzzy neural network model in analyzing the air pollution factors . . . . . 19*

*Dynamic phenomena in the active regions of 24-th solar cycle . . . . . 26*

*The optical afterglow observations of gamma-ray bursts . . . . . 31*

*Solar active phenomena observation . . . . . 32*

*Meteor observation in Irkutsk region . . . . . 33*

*Mongolian-Russian cooperation at the Khurel-Togoot observatory in the ison project framework . . . 34*

*A study of image prediction for yield mapping in real environment . . . . . 35*

***Geomagnetism . . . . . 41***

*Monitoring of the geomagnetic field variations at the high - mountain biospheric station dzhuga and forecasting of natural disasters and extreme weather . . . . . 43*

*Probing the Earth's mantle using satellite and ground - based magnetic data. Progress status and challenges . . . . . 44*

*Towards geophysical exploration of geothermal resources in the Hangai Mountains . . . . . 45*

*High-precision Overhauser magnetometers applications . . . . . 46*

*Variations of earthquake focal mechanism types in northern tien shan . . . . . 53*

*Tectonomagnetic monitoring of crustal stress state in the baikal rift zone and some results for study of the kultuk earthquake . . . . . 54*

*Rigid blocks in the earth's crust and strong earthquakes . . . . . 59*

*The monitoring of geomagnetic field in the Baikal-Hubsugul fault in 2010-2015 . . . . . 63*

*Geophysical complex ISTP SB RAS for monitoring electromagnetic fields in high and middle latitudes . . . . . 64*

*Study of the Magnetic Field Response due to Geodynamic Processes in Central Mongolia (Emeelt) and Russia (North-West Caucasus) . . . . . 65*

*The heat flows via CPD . . . . . 74*

***Geodynamics, active deformation, GPS, active fault, paleoseismology . . . . . 79***

*Identification and characterization of the Sharkhai and Avdar active faults near Mongolia's capital city: Impact on Seismic Hazard Assessment in a low deformation setting . . . . . 81*

*Co-seismic moment released by the surface rupturing 1934 bihar-nepal earthquake . . . . . 87*

*Stress fields in the area of the Mogod earthquake in Mongolia from the structural paragenetic analysis of tectonic fracturing . . . . . 88*

*Wave dynamics of rock deformations according results of monitoring . . . . . 94*

*Numerical reconstruction of normal-fault scarps evolution . . . . . 99*

*Radon monitoring of ulaanbaatar region . . . . . 103*

*Cosmogenic 36Cl geochronology of offset terraces along the Ovacık Fault (Malatya-Ovacık Fault Zone, Eastern Turkey): Implications for the intraplate deformation of the Anatolian Scholle . . . . . 104*

*Tropospheric delay of GPS signals and their connection with the level of moisture content within the Baikal region and the Selenga river basin . . . . . 105*

*Geodynamics of northern Mongolian and Transbaikalian segments of the Central Asian Orogenic Belt at*

*Late Paleozoic – Mesozoic* . . . . . 111
*GPS developments in mongolia and its applications in geodynamic studies* . . . . . 112
*Gheological hazard assessment of the Ulaanbaatar agglomeration* . . . . . 113
*Structural characterıstıcs of the Hovd fault zone, Mongolian Altaid regıon, western Mongolia* . . . . . 114
*Cumulative deformation by multiple surface-faulting earthquakes on the Bulnay Fault, Mongolia: A preliminary investigation* . . . . . 120
*Mapping of active faults in Korea by airborne LiDAR survey: A preliminary investigation* . . . . . 121
*Slip rates and ages of past earthquakes along the main western Gobi-Altay active slip faults (Gobi-Altay, Mongolia)* . . . . . 122
*Quantifying the differential uplift on the western branches of the north Anatolian fault: Sakarya river terraces, NW turkey* . . . . . 124
*Horizotal slip distribution through several seismic cycles the eastern Bogd fault, Gobi-Altai, Mongolia* . . . . . 129
*Impact of cosmic factors on the Baikal rift zone seismic regime* . . . . . 131
*Studying active faults by GPR technique; example of Songino fault Ulaanbaatar* . . . . . 137
*Present-day movements of the earth's crust of Mongolia from GPS measurements at the permanent sites* . . . . . 143
*First results of GPS measurements within the local networks in the Central Mongolia* . . . . . 147
*Songino active fault from GPR imaging and trench results, Ulaanbaatar, Mongolia* . . . . . 152
*The crustal state of stresses and the conditions of the tectonic structures activation of Southeast Mongolia in the Cenozoic* . . . . . 158
*Recurrence of strong earthquakes in the active Hovd fault zone, Mongolian Altay* . . . . . 163
*Tectonic position and geological manifestations of the 1967 Mogod earthquake, Mongolia* . . . . . 165
*Estimation of the recent activity of large faults in the Ulaanbaatar and Mogod geodynamic testing areas in Central Mongolia based on soil-radon data* . . . . . 166
*Active faults and Late Cenozoic crustal stress state in the central part of Mongolia* . . . . . 171
*Wave dynamics of seismicity in the annual cycles in the southeastern segment of the Amurian plate* . . . . . 176
*High-resolution surface rupture map and slip distribution of the 1905 M ≥ 8 Tsetserleg-Bulnay strike-slip earthquake sequence, Mongolia* . . . . . 181
*Intraplate geodynamics in Mongolia: constraints from geochronology, thermochronology, and geochemistry* . . . . . 182

***Large intra-continental earthquakes: Source characteristics, seismic activity, historical earthquakes*** . . . . . **183**
*Preliminary result of earthquake hypocenter determination using new 1d velocity model: khuvsugul area* . . . . . 185
*Seismicprofiling in a zone of mogod fault* . . . . . 186
*Mongolian National Seismic Network and its operations* . . . . . 189
*Lg-wave cross correlation applied to detection and location of events in high-seismicity regions of mainland east asia* . . . . . 190
*Earthquake Monitoring: Automatic processing at the Mongolian National Seismic Network* . . . . . 196
*Tectonophysical analysis of seismic hazard of faults in Central asia* . . . . . 197
*Focal mechanisms of aftershocks of Mw = 4.59, Bayanbulag earthquake* . . . . . 198
*A mechanism causing temporal variation in b-values Prior to a mainshock* . . . . . 199
*Ambient noise monitoring in Ulaanbaatar region* . . . . . 203
*Paleoseismic investigation on the eastern end of the Altyn Tagh fault* . . . . . 207
*Seismic activity of the Emeelt fault area investigated using tomoDD* . . . . . 208
*The seismicity of the south Hangay dome of central Mongolia: 1-d velocity model for the area from local earthquake data* . . . . . 209

*Radionuclide analysis of the CTBTO's IMS stations data in Mongolia . . . . . .210*
*Reference one dimensional velocity model and precise locations of local earthquake hypocenters in the hangay region . . . . . 211*
*Precise location of seismicity in and around Bulnay fault . . . . . 212*
*Detection capability of infrasound station . . . . . 213*
*Ground Penetrating Radar result of data analysis For Songino active fault, Ulaanbaatar . . . . . 214*
*Discrimination of earthquakes and explosions around north korean nuclear test site . . . . . .215*

***Crustal and lithosphere structures . . . . . 221***
*Deep structure of the baikal rift system Based on the seismic wave attenuation . . . . . .223*
*Deep velocity structure and anisotropic properties of the asian upper mantle . . . . . .228*
*Investigation of the boundary and internal fault zones of Tunka basin (Baikal rift system) using HVSR method . . . . . .231*
*High Topography and Deformation in Continental Interiors: Structure and Geodynamics of Central Mongolia . . . . . 235*
*Thickness of earth's crust under broadband stations of Mongolian seismic network . . . . . .236*
*Estimation of coda wave attenuation in the Hangay Dome, central Mongolia . . . . . .240*
*Crust and Upper Mantle Structure of Central Mongolia . . . . . 241*
*Receiver function imaging of crustal and upper mantle structure beneath seismic station Ulan-Ude (Transbaikalia, Russia) . . . . . 247*
*On conditions of preparation for the catastrophic earthquakes foci within earth crust of central asia . . . . . .250*
*Deep configuration of the southeast edge of the siberian craton along the passcal_1992 transect . . .256*
*Vibroseismic sounding of the earth's crust on the profile Baikal – Ulaanbaatar. . . . . .261*
*Study seismic activity in Khovd region (West part of Mongolia) and seismic velocity 1D model. . . . . 266*

***Seismic hazard assessment, strong ground motion, attenuation and site effects, microzoning 271***
*Seismic hazard assessment of bayan-ulgii aimag: Probabilistic analysis . . . . . 273*
*Seismic hazard assessment of bayan-ulgii aimag: Microzoning mapping . . . . . 277*
*Reducing Digitiser Latency for Earthquake Early Warning: New Strategies for Seismic Hardware. . 282*
*Prediction of seismic effects of large earthquakes in Mongolian-Siberian region by studying the dynamic parameters of earthquakes. . . . . .283*
*Paleoseismogenic deformations of the central Mongolia and seismic hazard assessment for Ulaanbaatar . . . . . 287*
*Site effect estimation of Bayan-Ulgii aimag . . . . . 288*
*Studying of tectonic infringements in seismically active areas of Mongolia. . . . . 290*
*Effects and Post-Disaster Actions during the 2015 Mw = 8.4 Northern Chile Earthquake. . . . . 295*
*Weather-climatic changes in the Baikal-Mongol region: analysis and forecast before 2050 . . . . . .296*
*The seismic microzoning study in Mongolia: the example of Ulgii city, center of Bayan-Ulgii aimag. . . . . 302*
*Seismic hazard assessment of bayan-ulgii aimag: Deterministic analysis . . . . . 306*
*Seismic safety assessment of earth dams. . . . . 309*
*Seismic microzoning on the joint of geotechnical lands-capes. . . . . 310*
*Seismic Microzonation: principles and practices (for example, the city of Ulan-Ude). . . . . 325*
*Cosmogenic 36Cl geochronology of offset terraces along the Ovacık Fault (Malatya-Ovacık Fault Zone, Eastern Turkey): Implications for the intraplate deformation of the Anatolian scholle . . . . . 330*